Nano-Self-Assembly of Nucleic Acids Capable of Transfection without a Gene Carrier

Kwang Suk Lim, Daniel Y. Lee, Gabriel M. Valencia, Young-Wook Won, and David A. Bull**

Nonviral gene carriers based on electrostatic interaction, encapsulation, or absorption require a large amount of polymer carrier to achieve reasonable transfection efficiencies. With cationic nanoparticles, for example, genes interact only with the surface of the nanoparticles, resulting in a low surface area to volume ratio (SA/$V = 3/r$). A large volume of carrier, therefore, is required to deliver a small copy number of genes. In this study, it is demonstrated that a nano-self-assembly of nucleic acids transfects itself into cells spontaneously, without the need for a gene carrier. The cellular uptake of this nanoassembly occurs through a number of endocytosis mechanisms. Once within the cell, the nanoassembly can escape endolysosomal vesicles and facilitate gene transfection. This nano-self-assembly consisting of zinc and plasmid DNA or siRNA, termed the Zn/DNA or Zn/siRNA nanocluster, is formed through the binding of Zn^{2+} ions to the phosphate groups of nucleic acids. The method described in this paper represents a new platform for carrier-free gene delivery that can be used to deliver any plasmid DNA or siRNA without the requirement for a specific modification in the nucleic acids or complicated steps to prepare dense particles.

1. Introduction

The development of nonviral gene carriers is based on one of the following principles: (1) electrostatic interaction, (2) encapsulation, and/or (3) absorption.[1–5] Each of these three principles, however, is also associated with the limitations of polymer carriers. First, cationic polymers may have an excessive charge density that correlates with increased toxicity of the polymer.[6,7] Alternative methods to reduce the amount of cationic polymer necessary to condense DNA or siRNA might minimize or eliminate the toxicity associated with these polymers.[8] Second, each of the methods of encapsulation is associated with one or more limitations: high shear stress, the exposure of nucleic acids to organic solvents, and extremely high temperatures.[9–11] Third, gene absorption involves adsorbing or conjugating cationic molecules, resulting in nucleic acids located on the surface of the carrier.[12,13] These nucleic acids present on the surface of the carrier are susceptible to enzymatic degradation.[13] New techniques to efficiently deliver siRNA have been developed to generate multimeric siRNA with an increased charge density[14] or to promote the self-assembly of elongated RNA strands into nano or microstructures.[7] Unfortunately, these techniques require the design of specific siRNA sequences or the modification of siRNA that makes it expensive to produce even small quantities of siRNA and cannot be applied to DNA delivery. Thus, there is a significant need for an alternative method of gene delivery that can be used to deliver either DNA or siRNA without the limitations inherent in viral or nonviral gene carriers.

For the nano-self-assembly of DNA or siRNA, we have focused on the interaction between divalent metal ions such as Zn^{2+}, Ca^{2+}, and Mg^{2+} and the phosphate groups in the nucleic acid backbone. This interaction forms intermolecular bridges connecting two or more phosphate groups, which drives the self-assembly of the nucleic acids (**Figure 1**a).[15,16] We hypothesized that the binding of these divalent metal ions to the phosphate backbone of DNA or siRNA could lead to the formation of a nanocluster, which could be internalized into cells by a variety of endocytosis mechanisms. The binding of the metal ions to the phosphate groups of the nucleic acids is reversible. The nanocluster of nucleic acids can be dissociated back into native DNA or siRNA and separate metal ions by lowering the pH because the structure of the nanocluster is maintained only within a pH range of 7.0–8.0.[17] This dependency on the pH of the local environment provides a basis for the endolysosomal escape of the nanocluster and subsequent gene transfection. Consequently, this nanocluster can serve as a platform for carrier-free gene delivery that is free of the limitations associated with both viral and nonviral gene carriers.

2. Results and Discussion

2.1. Formation of Divalent Metal Ion/Nucleic Acid Clusters

We examined whether the binding of the metal ions to the phosphate groups in the nucleic acid backbone drives the nano-self-assembly of DNA and siRNA. The mixtures of Zn/DNA,

K. S. Lim, D. Y. Lee, G. M. Valencia,
Dr. Y.-W. Won, Dr. D. A. Bull
Division of Cardiothoracic Surgery
Department of Surgery
University of Utah School of Medicine
Salt Lake City, UT 84132, USA
E-mail: yw.won@utah.edu; david.bull@hsc.utah.edu
D. Y. Lee, Dr. Y.-W. Won, Dr. D. A. Bull
Department of Pharmaceutics and Pharmaceutical Chemistry
University of Utah
Salt Lake City, UT 84112, USA

DOI: 10.1002/adfm.201502067

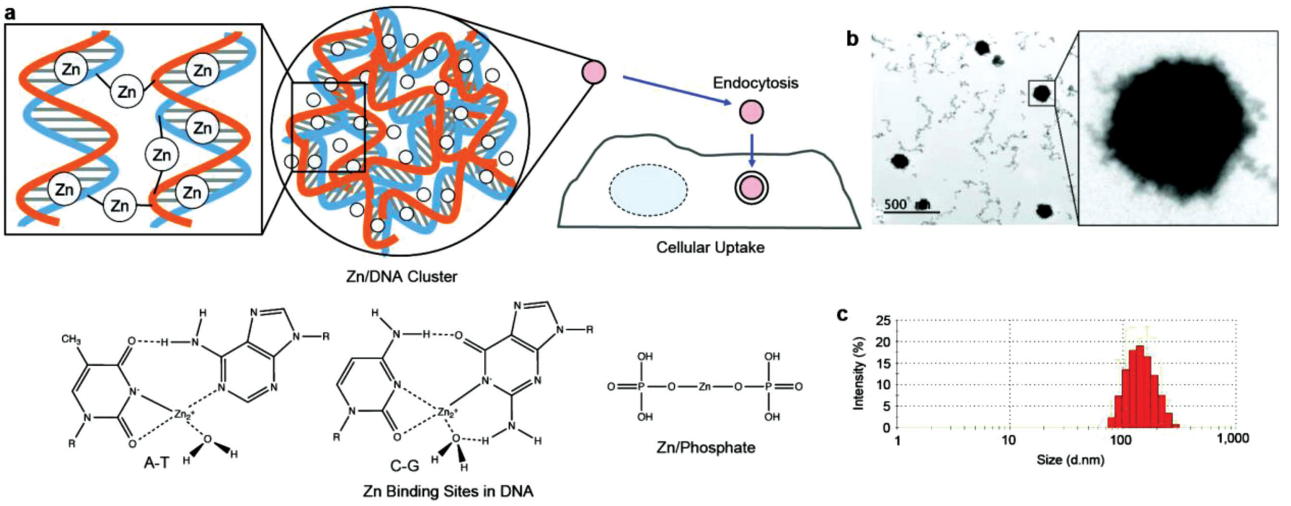

Figure 1. Schematic showing the process of formation of the Zn/DNA cluster, TEM images, and size distributions. a) Zn^{2+} bound to nitrogen in DNA base pairs condenses DNA and interacts with the phosphate groups to assemble DNA into the Zn/DNA cluster. The Zn/DNA cluster can internalize into cells by a number of endocytosis mechanisms. The Zn^{2+} present within the endolysosomal vesicle leads to an influx of counter ions and subsequent rupture of the vesicle. b) TEM image. c) The size distribution of the Zn/DNA cluster. The Zn/DNA cluster was prepared with 732×10^{-3} M $ZnCl_2$.

Ca/DNA, and Mg/DNA were electrophoresed to verify the formation of the nanocluster. Zn^{2+}, Ca^{2+}, and Mg^{2+} retarded the migration of DNA in a dose-dependent manner, meaning that they all led to the formation of a DNA nanocluster (Figure S1a,b in the Supporting Information and Figure 4a). In addition, Zn^{2+} and Mg^{2+} were able to condense siRNA, whereas Ca^{2+} precipitated out siRNA, and the Calcium Phosphate Transfection Kit did not retard siRNA (Figure S1c–e, Supporting Information).

To determine which divalent metal ion would be most suitable for gene transfection, we compared the cellular uptake of DNA or siRNA clustered by each of the metal ions. Among the three metal ions examined, Zn^{2+} was the metal ion that most effectively delivered DNA or siRNA into cells (**Figure 2**). More importantly, the Zn/DNA cluster demonstrated the highest levels of gene expression in the cells tested (Figure 2c,f). In addition, Zn^{2+} was the only divalent metal ion that was more efficient in facilitating the cellular uptake of nucleic acids than polyethyleneimine (PEI) 25 kDa, lipofectamine, and the Calcium Phosphate Transfection Kit (Figure 2g,h). These results suggest that the formation of the Zn/DNA or the Zn/siRNA cluster appears to be more efficacious in facilitating gene transfection than the nanoclusters formed with either Ca^{2+} or Mg^{2+}.

2.2. Characteristics of the Zn/DNA Cluster

Transmission electron microscopy (TEM) demonstrated that the interaction of Zn^{2+} with the phosphate backbone of DNA leads to the formation of the Zn/DNA cluster (Figure 1b), which has an average size of ≈200 nm (Figure 1c and Figure S2 in the Supporting Information) and a zeta potential of -12.9 ± 4.3 mV (pDNA: -29.6 ± 0.8 mV). The zeta potential of the Zn/DNA cluster is increased by the charge compensation of the DNA phosphate groups by Zn^{2+}.

The kinetics of the formation of the Zn/DNA cluster demonstrate that the self-assembly of DNA begins between a $ZnCl_2$ concentration of 145×10^{-3} and 293×10^{-3} M (**Figure 3**a). The fluorescence as a result of the intercalation of EtBr into DNA is continuously quenched over time because EtBr does not bind to the compact form of DNA. The optimum ratio of NaOH to Zn^{2+} to avoid the pH drop caused by the release of one proton per Zn^{2+} atom/base pair during the formation of the Zn/DNA cluster was determined (Figure S3, Supporting Information).[15] Measuring the absorbance at 260 nm, where the nitrogen absorbs the light, in the presence of $\geq 366 \times 10^{-3}$ M $ZnCl_2$ at a pH of 7.4, demonstrated a decrease in free DNA (Figure 3b,d), while no difference was observed at a pH of 5.0 (Figure 3c,d). This is the result of most of the nitrogen in the base pairs being consumed in the binding with Zn^{2+}. An assay to determine the free Zn^{2+} content revealed that the amount of Zn^{2+} present at a pH of 7.4 was lower than at a pH below 7.0 (Figure 3e). Free Zn^{2+} decreased with increasing pH and reached a steady state near a pH of 7.4, where the Zn/DNA cluster began to form (Figure 3f).

The binding of Zn^{2+} with the phosphate groups in the DNA backbone is the process driving the self-assembly of the nanocluster, which in turn retards the migration of the DNA (**Figure 4**a). Increasing the concentration of Zn^{2+} decelerates the DNA migration, resulting from the intermolecular bridges that connect each plasmid through the interaction of Zn^{2+} and phosphate. Since the binding of Zn^{2+} to the phosphate groups occurs only within a pH range of 7.0–8.0,[17] the assembly of DNA was not observed at a pH of 5.0 (Figure 4a). To verify the effects of the formation of the Zn/DNA cluster on DNA structure, HCl was added to dissociate the Zn/DNA cluster. The DNA band detected at the same location as the native DNA indicated that the Zn^{2+}/DNA binding was reversed at low pH, with DNA released without being cleaved as a result of the dissociation (Figure 4b).

2.3. In Vitro Transfection

To mimic in vitro transfection conditions, the Zn/DNA cluster was diluted in a physiologic buffer. The Zn/DNA cluster was

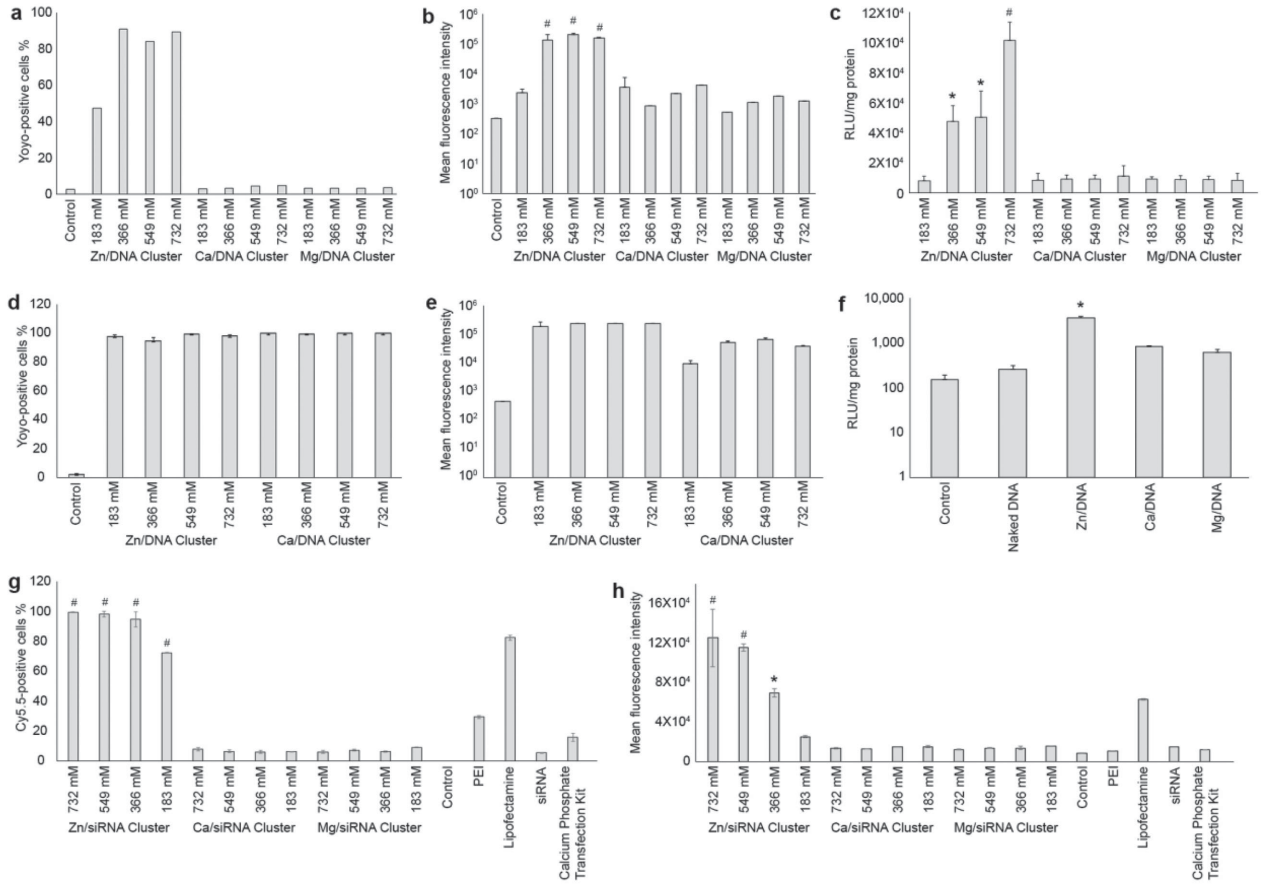

Figure 2. Comparison of the divalent metal ions. FACS analysis of the cellular uptake of yoyo-labeled DNA clustered by Zn^{2+}, Ca^{2+}, or Mg^{2+} into a,b) HEK293 cells or d,e) Jurkat T cells. c,f) Luciferase activity following the transfection of the Zn/DNA, the Ca/DNA, or the Mg/DNA clusters into c) HEK293 cells or f) A549 cells (366×10^{-3} M metal ions). g,h) Internalization of siRNA into HEK 293 cells delivered by the divalent metal ions, lipofectamine, cationic polymers, or the Calcium phosphate transfection kit. b,c,f,g,h) $\#p < 0.01$ versus Ca or Mg at the same concentration, $*p < 0.05$ versus Ca or Mg at the same concentration.

prepared in small volumes without NaOH or with NaOH to increase the pH to 7.4 and diluted into cell culture media. Regardless of the presence of NaOH, both conditions yielded the same results with regard to free DNA content and the EtBr fluorescence assay (Figure S4a,b, Supporting Information). The cell culture media used to dilute the Zn/DNA cluster had enough buffering capacity to facilitate or maintain the binding of Zn^{2+} with phosphate, demonstrating that adding NaOH is not necessary for in vitro transfection.

We investigated whether the Zn/DNA cluster could internalize into cells and transfect DNA in HEK293 cells.[18–20] Compared to naked DNA, the Zn/DNA cluster increased luciferase expression ≈1000-fold at a Zn^{2+} concentration of $\geq 549 \times 10^{-3}$ M, by 100-fold at a Zn^{2+} concentration of 366×10^{-3} M, and tenfold at a Zn^{2+} concentration of 183×10^{-3} M (Figure 4c), without significant cytotoxicity (Figure S5, Supporting Information). The transfection efficiency of the Zn/DNA cluster was more than 100× higher than PEI 1800 and more than 10× higher than poly-L-lysine (PLL), but tenfold lower than PEI 25 kDa. The Zn/DNA cluster was prepared with yoyo-labeled DNA to observe the cellular uptake. In the presence of $\geq 549 \times 10^{-3}$ M Zn^{2+}, ≈100% of cells were yoyo-positive (Figure 4d) and the fluorescence intensities were in direct proportion to the Zn^{2+} concentration (Figure 4e and Figure S6 in the Supporting Information). Although the cellular uptake of DNA delivered through the formation of the Zn/DNA cluster was the most efficient, PEI 25 kDa showed the highest levels of gene expression (Figure 4c–e). This could be due to strong DNA protection and facilitated endosomal escape by PEI. One of the advantages of the Zn/DNA cluster over PEI is that it can deliver genes into ≈100% of cells, while PEI delivers genes into only 40% of the cell population (Figure 4d).

2.4. Mechanistic Studies

The detailed pathways of the internalization of the Zn/DNA cluster need to be defined because the mechanism of internalization determines the intracellular processing of the Zn/DNA cluster and the subsequent transfection efficiency. The DNA internalized into the nucleus and spread throughout the entire cytosol within an hour when the Zinc/DNA cluster was prepared at a concentration of 732×10^{-3} M Zn^{2+}, while the fluorescence in the groups at 183×10^{-3} M Zn^{2+} or 366×10^{-3} M Zn^{2+}

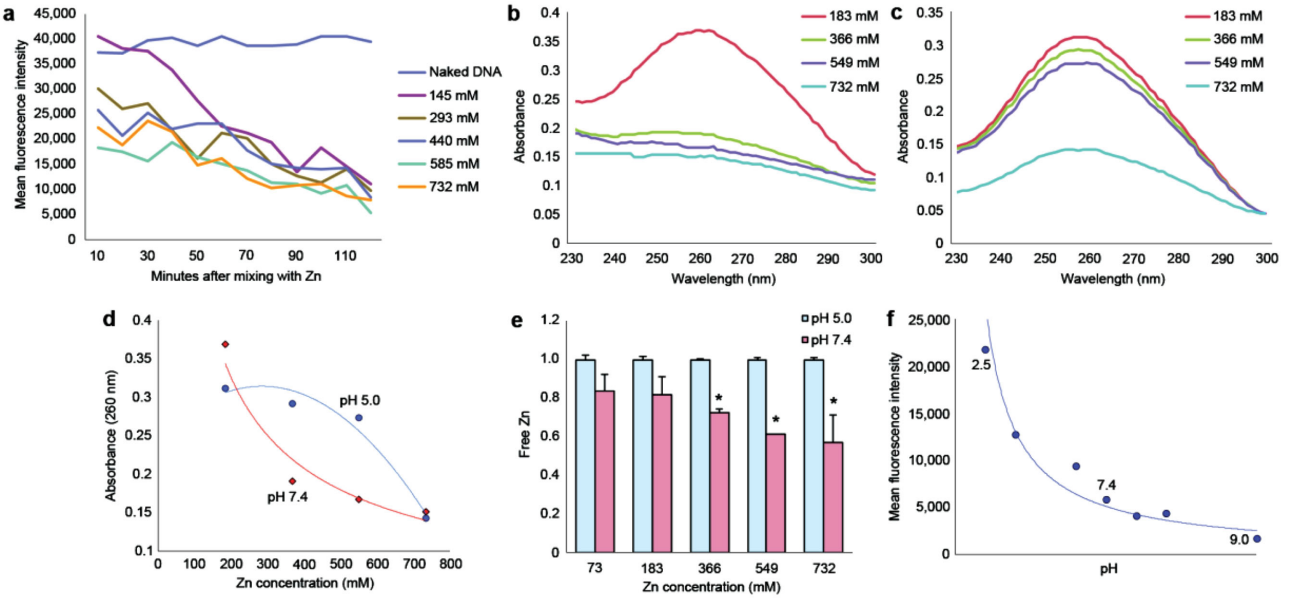

Figure 3. Confirmation of the binding of Zn^{2+} to DNA. a) Binding of Zn^{2+} to DNA as observed by EtBr replacement assay. Free DNA in the presence of different concentrations of Zn^{2+} was determined by measuring the absorbance at b) pH 7.4 or c) pH 5.0. d) Patterns representing changes in the free DNA content as a function of the Zn^{2+} concentration at a pH of 7.4 or at a pH of 5.0 were obtained by recording the absorbance values at 260 nm. e) Free Zn^{2+} content in the Zn/DNA cluster was determined at a pH of 7.4 or at a pH of 5.0 (*$p < 0.05$ vs pH 5.0). f) Changes in free Zn^{2+} mixed with DNA as a function of pH.

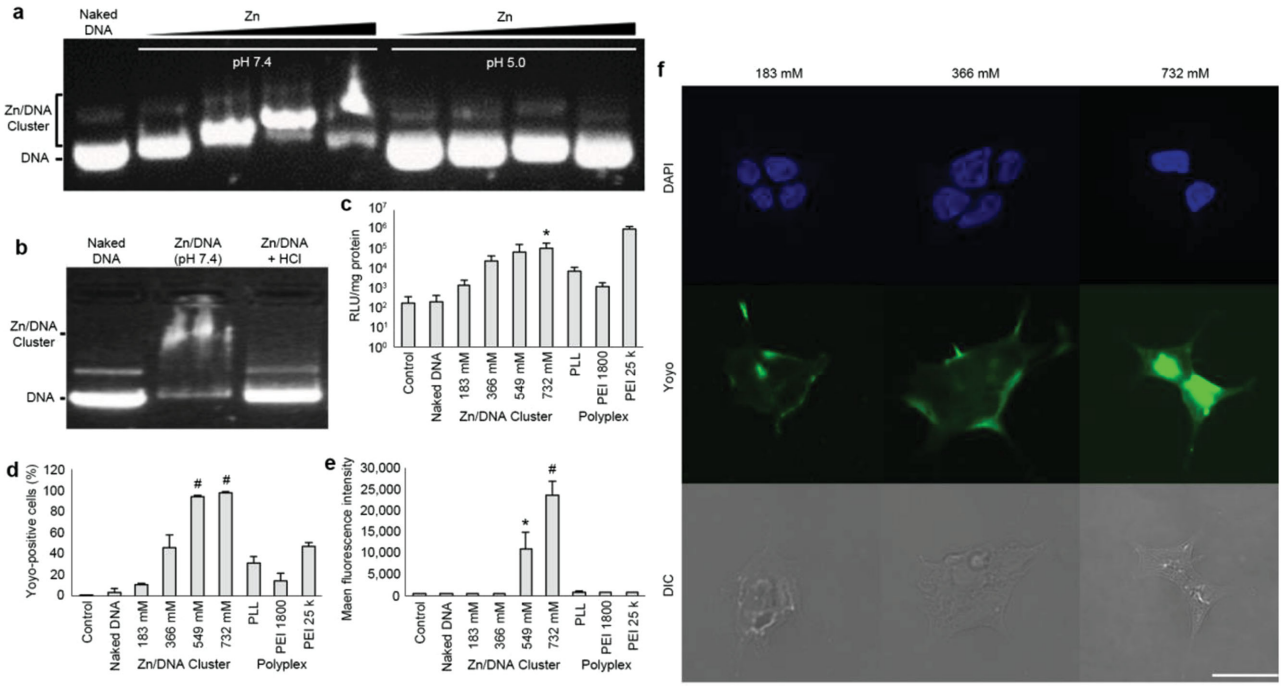

Figure 4. Confirmation of the formation of the Zn/DNA cluster, in vitro transfection, and cellular uptake of the Zn/DNA cluster. a) The formation of the Zn/DNA cluster observed by gel retardation assay. b) Reversibility of the Zn/DNA cluster at low pH. a,b) The Zn/DNA clusters were prepared with 732×10^{-3} M $ZnCl_2$. c) Luciferase gene transfection by the Zn/DNA cluster (*$p < 0.05$ vs PLL or PEI1800). Cellular uptake of the Zn/DNA cluster determined by FACS analysis representing d) the percentage of yoyo-positive cells and e) the mean fluorescence intensity in each of the cells (#$p < 0.01$ vs PLL, PEI1800, or PEI25 k; *$p < 0.05$ vs PLL, PEI1800, or PEI25 k). f) Confocal image showing the internalization of the Zn/DNA cluster prepared with different Zn^{2+} concentrations. Cells were treated with the Zn/DNA cluster for 1 h. Scale bar: 10 μm. The Zn^{2+} concentrations indicate the concentrations of $ZnCl_2$ used to prepare the Zn/DNA cluster before the dilution (1/100) with the culture media.

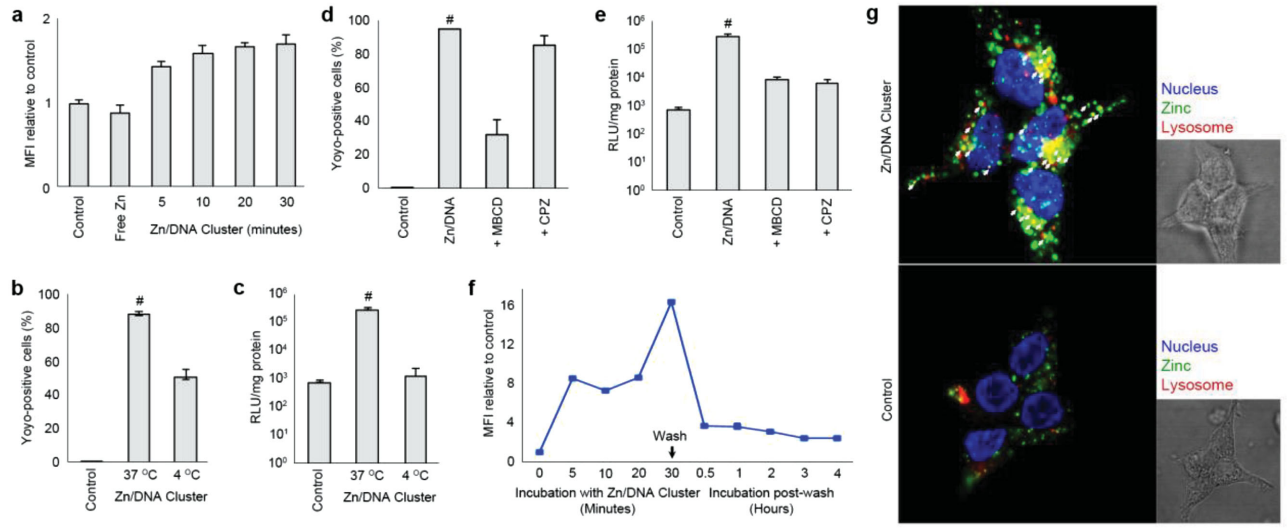

Figure 5. Mechanism of internalization of the Zn/DNA cluster. a) Zn^{2+} content in the cells. Cells were treated either with the Zn/DNA cluster in a time-dependent manner or with $ZnCl_2$. The concentration of $ZnCl_2$ was equivalent to Zn^{2+} in the Zn/DNA cluster, and cells were incubated with $ZnCl_2$ for 30 min. b,c) Effect of temperature on cellular uptake and gene transfection. b) The internalization of the Zn/DNA cluster and c) the transfection efficiency of the Zn/DNA cluster in cells cultured at 37 °C or 4 °C ($\#p < 0.01$ vs 4 °C). d,e) Cellular uptake and gene transfection of the Zn/DNA cluster in the presence of endocytosis inhibitors. d) Yoyo-positive cells ($\#p < 0.01$ vs MβCD) and e) luciferase expression levels ($\#p < 0.01$ vs MβCD or CPZ). f) Kinetics of Zn^{2+} clearance from the cells. f) Confocal image showing colocalization of the Zn/DNA cluster with lysosomes (white arrows). Nucleus stained blue by DAPI, Zn^{2+} detected as green by FluoZin-3, and lysosome labeled red. The Zn/DNA clusters were prepared with 732×10^{-3} M $ZnCl_2$.

was detected near the cell membrane (Figure 4f). We investigated whether the kinetics of the cellular recruitment of Zn^{2+} are correlated to those of the uptake of the Zn/DNA cluster. Cellular Zn^{2+} content increased in a time-dependent manner, whereas uptake of Zn^{2+} was not observed when cells were incubated with free $ZnCl_2$ (**Figure 5**a and Figure S7 in the Supporting Information), indicating that the increased Zn^{2+} level in the cells was due to the internalization of the Zn/DNA cluster. Moreover, treatment of naked DNA in the presence of the same $ZnCl_2$ concentration used to prepare the Zn/DNA cluster could not increase the gene expression (relative luminescence unit (RLU) without $ZnCl_2$: 517.9 ± 25.0, with $ZnCl_2$: 586.0 ± 58.0), meaning that the enhanced gene expression was due to the uptake of the Zn/DNA cluster, not the addition of $ZnCl_2$.

Nonphagocytic endocytosis, in particular pinocytosis, is known to be the primary route of cell entry for nonviral gene carriers.[21,22] Pinocytosis can be subdivided into macropinocytosis, clathrin-dependent endocytosis (CDE), and clathrin-independent endocytosis (CIE).[23] An assessment of the contribution of each pathway to the overall mechanism of internalization of the Zn/DNA cluster is essential for understanding the increased gene transfection facilitated by the Zn/DNA cluster. When the Zn/DNA cluster was transfected at 4 °C, the cellular uptake and the gene expression decreased by ≈50% compared to the gene expression found at 37 °C (Figure 5b,c and Figures S8 and S9 in the Supporting Information), demonstrating that endocytosis is involved in the cellular uptake of the Zn/DNA cluster. Confocal microscopy further verified that some of the Zn/DNA clusters were found inside the lysosomes and that the Zn^{2+} content in the cells increased compared to the control group (Figure 5g).

Chlorpromazine (CPZ; CDE inhibitor) and methyl-β-cyclodextrin (MβCD; CIE inhibitor) were used to assess which endocytosis pathway was the primary uptake mechanism for the Zn/DNA cluster.[24,25] The presence of a CDE inhibitor or a CIE inhibitor is known to reduce the uptake of particles with a hydrodynamic diameter of ≈200 nm or ≈100 nm, respectively.[25] Compared to the groups without the inhibitors, the cellular uptake of the Zn/DNA cluster decreased to 85% in the presence of CPZ and to 30% in the presence of MβCD (Figure 5d and Figure S10 in the Supporting Information). Since the copy number of DNA or the amount of Zn/DNA cluster present in the cells is in direct proportion to the mean fluorescence intensity of yoyo-dye or FluoZin-3, respectively, this result indicates that a lower quantity of DNA was internalized into the cells in the presence of the CIE inhibitor than in the presence of the CDE inhibitor (Figures S10 and S11, Supporting Information). Interestingly, although a different quantity of DNA internalized in the presence of either CPZ or MβCD, the level of gene expression decreased by 30% in both cases (Figure 5e and Figures S10 and S11 in the Supporting Information). This result was not due to any toxicity of the inhibitors (Figure S12, Supporting Information). The smaller Zn/DNA cluster (<100 nm) internalized more efficiently, but its transport into the nucleus was not as efficient as the larger Zn/DNA cluster (<200 nm). Since the smaller Zn/DNA cluster contained a smaller number of Zn^{2+} ions, the endolysosomal concentration of Zn^{2+} may not have been high enough to induce an influx of counter ions to rupture the vesicle.

TEM was conducted to investigate whether macropinocytosis, direct transduction, or other pathways contributed to the internalization of the Zn/DNA cluster (**Figure 6**). The TEM image illustrates that macropinocytosis is one of the mechanisms of internalization and that the Zn/DNA cluster can escape the endolysosomal vesicles (Figure 6a–e). Surface-connected tubular invaginations and direct transport were also observed

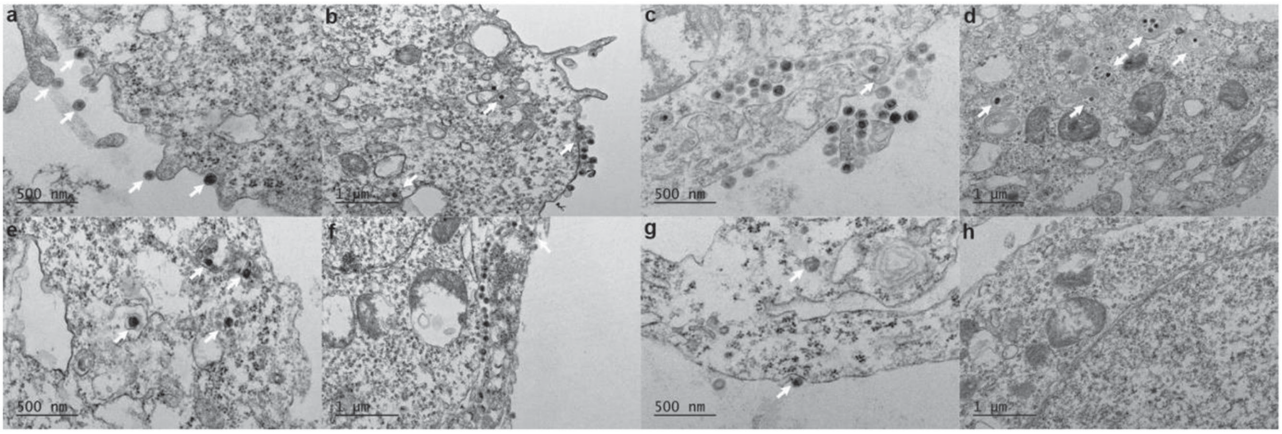

Figure 6. TEM images showing modes of internalization of the Zn/DNA cluster into HEK293 cells. a) Formation of macropinosomes ruffles the cell surface into open cups followed by b) ruffle closure, c) cup closure, and d) the intracellular vesicles. Ruffle closure and cup closure are defined as a circular cup of plasma membrane and the separation of the macropinosome from the plasma membrane, respectively. Arrows indicate a) locations of the Zn/DNA cluster near the cell membrane and b,d) the Zn/DNA cluster in endolysosomal vesicles. e) The rupture of endolysosomal vesicles. Arrows indicate the endolysosomal vesicles, which contain the Zn/DNA cluster, being destroyed. Other mechanisms of internalization of the Zn/DNA cluster, including f) surface-connected tubular invaginations and g) direct transport. h) Control.

to be involved in the internalization of the Zn/DNA cluster (Figure 6f,g). These results clearly demonstrate that macropinocytosis, CDE, CIE, and direct transduction all contribute to the cellular uptake of the Zn/DNA cluster. It is however difficult to define which of these is the primary mechanism of internalization of the Zn/DNA cluster and conclude that the mechanisms involved in the internalization of the Zn/DNA cluster into HEK293 cells can be broadly applied to other types of cells because the mechanism of nanoparticle endocytosis is specific to cell type.

2.5. Clearance of Zn^{2+}

We studied the kinetics of the clearance of Zn^{2+} from HEK293 cells because an increase in intracellular Zn^{2+} inhibits enzymatic activity and the sustained exposure of cells to high levels of Zn^{2+} induces apoptosis.[26] The content of intracellular Zn^{2+} increased continuously in the first 30 min of cell incubation with the Zn/DNA cluster and decreased dramatically within 30 min following washing and additional incubation (Figure 5f). The sum amount of Zn remained inside the cells and Zn secreted to the culture media was calculated to be almost the same as the quantity of Zn treated to the cells. The TEM image also showed that the Zn/DNA cluster disappeared at 30 min postincubation after washing the Zn/DNA cluster (Figure S13, Supporting Information). These results demonstrate that Zn^{2+} is cleared rapidly from cells to maintain cellular homeostasis of Zn^{2+}.

3. Conclusion

The development of a reliable and stable method of carrier-free gene delivery would greatly reduce the risk profile of clinical gene therapy by eliminating the toxicity associated with viral vectors and nonviral gene carriers. This study addresses a carrier-free gene delivery method that can be used to deliver any type of DNA or siRNA without the requirement for a specific modification in the nucleic acids or complicated steps to prepare dense particles. We have proven our hypothesis that the interaction between divalent metal ions and the phosphate backbone of DNA or siRNA drives the formation of a nano-self-assembly of DNA or siRNA, which can internalize into cells. Zn^{2+} is the most optimal metal ion for the formation of the nanocluster among those tested in this study. The Zn/DNA or the Zn/siRNA cluster can deliver DNA or siRNA, respectively, without the requirement for a gene carrier, a specific modification in the nucleic acids, or complicated steps to prepare dense particles. We have demonstrated that DNA clustered by Zn^{2+} internalizes into cells by a number of endocytosis mechanisms and escapes the endosome due to the increased concentration of Zn^{2+} present, meaning that the Zn/DNA cluster allows the efficient and homogeneous delivery of a large copy number of nucleic acids into cells. Although it has been clearly demonstrated that this nanocluster is capable of facilitating DNA expression or siRNA uptake in a variety of cell types, gene knockdown by siRNA delivery through the formation of the Zn/siRNA cluster remains a future challenge.

4. Experimental Section

Materials: $ZnCl_2$, $CaCl_2$, $MgCl_2$, CPZ, MβCD, MTT, PLL, and PEI were purchased from Sigma-Aldrich (St. Louis, MO). A plasmid DNA expressing luciferase and a luciferase assay kit were obtained from Promega (Madison, WI). Cy5.5-labeled noncoding siRNA was synthesized by the Nucleic Acid Core Facility at the University of Utah (Salt Lake City, UT). The Calcium Phosphate Transfection Kit, all cell culture supplies, FluoZin-3, and pHrodo dye were purchased from Life Technologies (Invitrogen, Grand Island, NY).

Preparation and Characterization of the Nanocluster: Ten micrograms of DNA or siRNA was mixed with different concentrations of $ZnCl_2$, $CaCl_2$, or $MgCl_2$, and the pH of the mixture was adjusted to 7.4 by adding predetermined amounts of NaOH. The mixture of DNA or siRNA and each of the metal ions was incubated for 20 min to formulate the

nanocluster. The nanocluster was further diluted in phosphate buffered saline (PBS) or cell culture media before use. Retarded migration of DNA or siRNA resulting from the formation of the nanocluster was confirmed by agarose gel electrophoresis. The formation of the Zn/DNA clusters was confirmed by TEM (JEOL JEM-1400 Plus). The size distribution and the zeta potential of the Zn/DNA cluster were determined by dynamic light scattering (Malvern Zetasizer Nano-ZS; Malvern Instruments) with three parallel measurements.

Confirmation of the Zn/DNA Binding: The condensation of DNA by the binding of Zn^{2+} to phosphates was verified by an EtBr exclusion assay. To determine the initial fluorescence, the mixture of 10 μg DNA and EtBr was incubated for 15 min and the intensity was recorded. $ZnCl_2$ was added to the mixture at the predetermined concentration and the fluorescence quenching was observed continuously over time. Free DNA was determined by scanning absorbance values in the presence of different concentrations of $ZnCl_2$. Free Zn^{2+} content was calculated by using FluoZin-3 according to the manufacturer's instructions.

Cell Culture: HEK293, Jurkat T, and A549 cells were maintained according to the protocols provided by the ATCC. Jurkat T cells and A549 cells were chosen to normalize the transfection efficiency of the Zn/DNA cluster because Jurkat T cell is widely accepted as a difficult-to-transfect cell line and A549 is a commonly used cancer cell line in gene transfection studies.[27,28] HEK293 cells were used in most of the luciferase transfection experiments, the mechanistic studies, and the TEM observations because this cell line has been extensively used as a test tool for gene transfection for over 25 years and retains machinery for most of the post-translational modification and generating functional, mature proteins originated from both mammalian and nonmammalian genes.[29,30]

Transfection and Cellular Uptake: Ten micrograms of DNA labeled with the yoyo-dye or 10 μg Cy5.5-labeled siRNA was processed to form the Zn/DNA or the Zn/siRNA cluster with different concentrations of $ZnCl_2$. HEK293, Jurkat T, and A549 cells treated with the Zn/DNA or the Zn/siRNA cluster for 30 min were prepared for flow cytometry (FACSCanto, BD Bioscience; Heidelberg, Germany) and confocal microscopy (Nikon A1R Confocal Microscope). For the in vitro transfection, the Zn/DNA cluster was prepared with DNA encoding luciferase. Each well of 24-well plate received 1 μg DNA or 1 μg siRNA. The cells treated with the Zn/DNA cluster prepared at different concentrations of Zn, the DNA/PLL polyplex prepared at a 1/4 weight ratio, the DNA/PEI1800 polyplex prepared at a 1/8 weight ratio, or the DNA/PEI25k prepared at a 1/1 weight ratio were incubated for 48 h, and the luciferase activity in the cell lysates was determined according to the manufacturer's protocol. An 3-(4,5-dimethylthiazol-2-yl)-2,5-diphenyltetrazolium bromide (MTT) assay was performed to determine the cell viability.

Mechanistic Studies: HEK293 cells were preincubated with 17×10^{-3} M CPZ or 2.5×10^{-3} M MβCD 6 h prior to the treatment of the Zn/DNA cluster. The Zn/DNA cluster was prepared with 20 μg DNA in the presence of 366×10^{-3} M ZnCl and further diluted down to 1/100 by adding cell culture media containing 1×10^7 cells. After 30 min of incubation, cells were washed thoroughly and fixed immediately. To demonstrate the dissociation of the Zn/DNA cluster, the cells were incubated for an additional 30 min after the washing, followed by fixing. The cells were then processed for analysis and observation by TEM.

Zn Clearance: The Zn/DNA cluster was prepared with 20 μg DNA in the presence of 366×10^{-3} M ZnCl, and the Zn/DNA cluster containing 1 μg DNA was transfected to each well of 24-well plate containing 4×10^4 HEK293 cells on the day after the cell seeding. The final volume of the Zn/DNA cluster treated was 20% of the culture media. To determine the intracellular or extracellular concentrations of free Zn at different time points, cell lysates and cell culture media were collected at the predetermined time points. The levels of free Zn were determined by using FluoZin-3 according to the manufacturer's instruction.

Supporting Information

Supporting Information is available from the Wiley Online Library or from the author.

Acknowledgments

Y.W.W. and D.A.B. contributed equally to this work.

Received: May 19, 2015
Revised: June 19, 2015
Published online: July 28, 2015

[1] K. A. Whitehead, R. Langer, D. G. Anderson, *Nat. Rev. Drug Discovery* **2009**, *8*, 129.
[2] D. W. Pack, A. S. Hoffman, S. Pun, P. S. Stayton, *Nat. Rev. Drug Discovery* **2005**, *4*, 581.
[3] S. Y. Wong, J. M. Pelet, D. Putnam, *Prog. Polym. Sci.* **2007**, *32*, 799.
[4] T. G. Park, J. H. Jeong, S. W. Kim, *Adv. Drug Delivery Rev.* **2006**, *58*, 467.
[5] D. Putnam, *Nat. Mater.* **2006**, *5*, 439.
[6] J. Zhou, J. Liu, C. J. Cheng, T. R. Patel, C. E. Weller, J. M. Piepmeier, Z. Jiang, W. M. Saltzman, *Nat. Mater.* **2012**, *11*, 82.
[7] J. B. Lee, J. Hong, D. K. Bonner, Z. Poon, P. T. Hammond, *Nat. Mater.* **2012**, *11*, 316.
[8] R. Kanasty, J. R. Dorkin, A. Vegas, D. Anderson, *Nat. Mater.* **2013**, *12*, 967.
[9] S. Ando, D. Putnam, D. W. Pack, R. Langer, *J. Pharm. Sci.* **1999**, *88*, 126.
[10] E. Walter, K. Moelling, J. Pavlovic, H. P. Merkle, *J. Controlled Release* **1999**, *61*, 361.
[11] D. Wang, D. R. Robinson, G. S. Kwon, J. Samuel, *J. Controlled Release* **1999**, *57*, 9.
[12] M. Singh, M. Briones, G. Ott, D. O'Hagan, *Proc. Natl. Acad. Sci. USA* **2000**, *97*, 811.
[13] S. Munier, I. Messai, T. Delair, B. Verrier, Y. Ataman-Onal, *Colloids Surf., B* **2005**, *43*, 163.
[14] H. Mok, S. H. Lee, J. W. Park, T. G. Park, *Nat. Mater.* **2010**, *9*, 272.
[15] P. Aich, S. L. Labiuk, L. W. Tari, L. J. Delbaere, W. J. Roesler, K. J. Falk, R. P. Steer, J. S. Lee, *J. Mol. Biol.* **1999**, *294*, 477.
[16] D. O. Wood, M. J. Dinsmore, G. A. Bare, J. S. Lee, *Nucleic Acids Res.* **2002**, *30*, 2244.
[17] C. M. Muntean, K. Nalpantidis, I. Feldmann, V. Deckert, *Spectroscopy* **2009**, *23*, 155.
[18] J. A. Kim, C. Aberg, A. Salvati, K. A. Dawson, *Nat. Nanotechnol.* **2012**, *7*, 62.
[19] A. Salvati, C. Aberg, T. dos Santos, J. Varela, P. Pinto, I. Lynch, K. A. Dawson, *Nanomedicine* **2011**, *7*, 818.
[20] C. He, Y. Hu, L. Yin, C. Tang, C. Yin, *Biomaterials* **2010**, *31*, 3657.
[21] R. Wattiaux, N. Laurent, S. Wattiaux-De Coninck, M. Jadot, *Adv. Drug Delivery Rev.* **2000**, *41*, 201.
[22] L. K. Medina-Kauwe, J. Xie, S. Hamm-Alvarez, *Gene Ther.* **2005**, *12*, 1734.
[23] S. D. Conner, S. L. Schmid, *Nature* **2003**, *422*, 37.
[24] D. Vercauteren, R. E. Vandenbroucke, A. T. Jones, J. Rejman, J. Demeester, S. C. De Smedt, N. N. Sanders, K. Braeckmans, *Mol. Ther.* **2010**, *18*, 561.
[25] R. A. Petros, J. M. DeSimone, *Nat. Rev. Drug Discovery* **2010**, *9*, 615.
[26] A. Krezel, W. Maret, *J. Am. Chem. Soc.* **2007**, *129*, 10911.
[27] J. F. Kukowska-Latallo, A. U. Bielinska, J. Johnson, R. Spindler, D. A. Tomalia, J. R. Baker Jr., *Proc. Natl. Acad. Sci. USA* **1996**, *93*, 4897.
[28] W. Guang Liu, K. De Yao, *J. Controlled Release* **2002**, *83*, 1.
[29] P. Thomas, T. G. Smart, *J. Pharmacol. Toxicol. Methods* **2005**, *51*, 187.
[30] Y. C. Lin, M. Boone, L. Meuris, I. Lemmens, N. Van Roy, A. Soete, J. Reumers, M. Moisse, S. Plaisance, R. Drmanac, J. Chen, F. Speleman, D. Lambrechts, Y. Van de Peer, J. Tavernier, N. Callewaert, *Nat. Commun.* **2014**, *5*, 4767.